journal

J. Am. Ceram. Soc., 76 [6] 1445–51 (1993)

Transient Plastic Phase Processing of Titanium–Boron–Carbon Composites

Michel W. Barsoum* and Boen Houng*

Department of Materials Engineering, Drexel University, Philadelphia, Pennsylvania 19104

Ceramic/ceramic composites in the Ti–B–C system were fabricated by a novel process referred to as transient plastic phase processing (TPPP). The basic concept is based on the following reaction:

"soft" transient plastic matrix

+ reactant phase → hard matrix

+ reinforcement phase

where the transient plastic phase is a phase with a wide range of stoichiometry and a yield point that is a strong function of that stoichiometry. The reactant phase is one that will react with the transient phase in such a way so as to shift the composition of the latter toward its harder and more refractory composition. The composite is formed in two stages: In the first, pressure is applied to shape and fully densify the reactants while the transient phase is soft, i.e., before reaction. Once the reactants are densified, the reaction is allowed to proceed, forming a new phase and rendering the matrix more refractory. If the volume change upon reaction is small, then the density of the final compact will remain near theoretical. Using this approach ceramic/ceramic composites in the Ti–B–C system were hot-pressed to full density and complex shapes at temperatures as low as 1600°C.

I. Introduction

THE demand for materials exhibiting exceptional hardness and stability at very high temperatures has led to a renewed interest in refractory materials such as the carbides, borides, beryllides, nitrides, and silicides. Other potential applications for this class of materials include armor plates, cutting tools, and dies. Beyond these properties the ability to fabricate fully dense ultrarefractory ceramic/ceramic composites could result in a new class of materials that exhibit unique and attractive combinations of mechanical, electrical, and magnetic properties.

TiB_2 is representative of refractory compounds with very high melting points and high hardness. Ramberg *et al.*[1] have shown that fine-grained ultrapure TiB_2 possesses extraordinary resistance to plastic deformation at high temperatures, which they concluded was a result of the existence of a high Peierls stress, i.e., intrinsic to the material. Furthermore, the fracture toughness of roughly 5 $MPa \cdot m^{1/2}$ is also encouraging. In contrast, TiC deforms plastically over the range 1000–1500°C.[2] TiC, however, can be precipitation hardened by TiB_2 at high temperatures by the addition of a fraction of a percent of B.[2] This combination of extreme resistance to plastic deformation, precipitation hardening, and the high-temperature plasticity of the TiC phase suggests that a TiB_2–TiC composite should be attractive as a high-temperature structural ceramic. Other potential applications include armor, dies, machine tool inserts, and, given their good electrical conductivity, cathodes in Hall–Heroult cells for the electrolytic production of aluminum.

Inasmuch as these refractory materials not only are themselves among the hardest available, but possess melting temperatures among the highest known, processing them into complex shapes and full densities requires extremely high sintering temperatures and poses a veritable challenge. For example, hot-pressing of TiB_2 and TiC at 2200°C, 10 MPa for 15 min, yielded samples that were between 95% and 97% dense.[3]

The processing challenge has been circumvented in a variety of processing techniques which include the following: starting with ultrafine plasma-arc-derived powders;[4] the addition of large amounts of sintering aids;[5–7] cemented carbides, self-propagating high-temperature synthesis;[8,9] and more recently by a direct liquid Zr metal–B_4C reaction.[10] In this last process the Zr is molten and allowed to react with a B_4C preform.

In this paper, a new and novel technique termed transient plastic phase processing (TPPP) is introduced for the fabrication of ultrarefractory ceramic/ceramic composites to full density and complex net shapes at relatively low homologous temperatures.

II. Conceptual Approach

Ideally materials should be processed in a soft ductile condition and then strengthened by heat treatment, an approach that is fundamental in metallurgy. This concept has also been applied to ceramic materials. A classic example is provided by the glass-ceramic industry: parts are formed and shaped from the melt and subsequently heat-treated to crystallize the glass into a more refractory and tougher material. Another example is transient liquid-phase sintering. More recently transient viscous sintering[11] has been shown to facilitate the fabrication of mullite and mullite composites. In each case the idea is the same: processing in the presence of a viscous, easily formable phase, after which that phase is removed by either crystallization or reaction.

By analogy with these methods we propose TPPP for the fabrication of ceramic/ceramic composites. The process involves a solid-state reaction between two (or more) phases in particulate form in which one is a transient plastic phase (TPP) and another is a reactant phase (RP). The TPP is nonstoichiometric with a range of stoichiometry and for which the yield point is a strong function of stoichiometry. The RP reacts with the TPP and shifts the stoichiometry of the latter toward a harder and more refractory stoichiometry.

To illustrate the basic principles and steps involved in TPPP, a schematic of the process is illustrated in Fig. 1. The starting constituents are AC_2, which is the RP, and AB_x, which is the TPP. An isothermal section of the corresponding ABC ternary phase diagram at the reaction temperature is shown in Fig. 2(a). In this case, the A-rich compositions of the AB_x are assumed to have lower yield strengths than the B-rich compositions along the binary AB composition axis of the ternary diagram.

R. Ruh—contributing editor

Manuscript No. 195416. Received August 12, 1992; approved January 19, 1993.

*Member, American Ceramic Society.

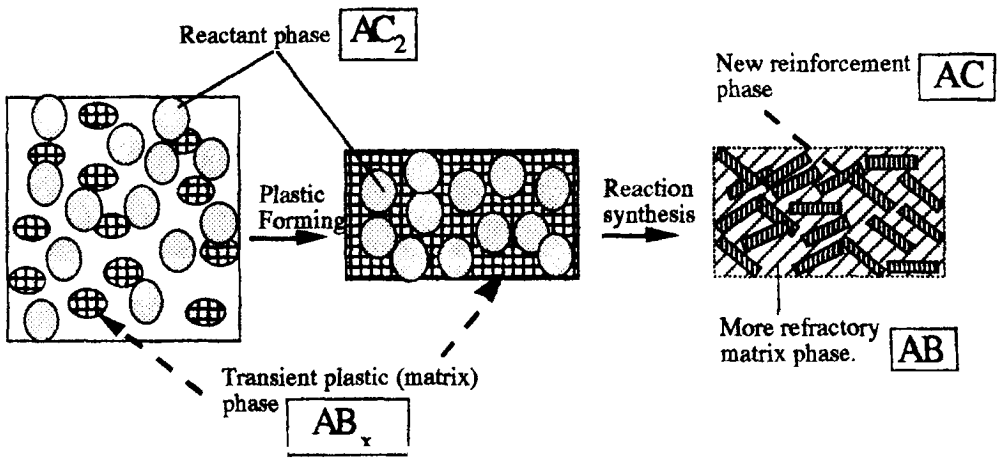

Fig. 1. Schematic of steps involved during transient plastic phase processing. In the first stage use is made of the "softness" of the transient phase to obtain a fully dense body. Upon reaction the composition of the transient phase shifts toward the harder more refractory composition.

The two phases in powder form are mixed and hot-pressed, extruded, or forged. The ductility of AB_x prior to the reaction (i.e., A-rich) ensures that the compact will achieve full density with the required net or near-net shape. Following this initial densification step in TPPP, the reaction is of the form

$$RP + TPP \rightarrow \text{reinforcing phase} + \text{ceramic matrix} \quad (1)$$

With specific reference to Fig. 2(a), the reaction is

$$(1 - x)AC_2 + AB_x \rightarrow 2(1 - x)AC + xAB \quad (2)$$

where AC is now the reinforcing phase and AB is the refractory matrix phase in the resulting ceramic/ceramic composite. As reaction (2) proceeds, the stoichiometry of the TPP shifts towards the B-rich side of the binary line AB and the TPP becomes more refractory. This reaction depletes the TPP of the element A that renders it ductile.

The two key steps in TPPP and the resulting microstructures are illustrated in Fig. 1. Plastic forming results in densification of the mix of powders (AC_2 and AB_x) with essentially no change in the composition of the phase constituents. During reaction synthesis, compositions change, resulting in the formation of a ceramic/ceramic composite consisting of the new reinforcing phase AC in a refractory matrix of composition AB.

The following conditions must be met for successful TPPP:

(i) The reaction rate has to be slower than the time needed for consolidation. This condition is met if the TPP is relatively ductile at higher temperatures and the reaction rates involved are slow. The time for consolidation will clearly depend on the applied stress and the creep properties of the TPP.

(ii) The volume change upon reaction has to be small (<1%) or preferably positive. Since the reactions of interest are usually exothermic, the overall volume change upon reaction will normally be negative,[12] which in turn gives rise to internal porosity in the final product. If the amount of shrinkage is small, it could easily be eliminated by moderate pressure or by a high-temperature anneal. Since the shrinkage associated with the reaction synthesis when the RP is in elemental form is characteristically high,[12] the RP phases in the form of compounds are preferred.

(iii) The standard free energy of reaction has to be negative. This is easily determined by examination of the compatibility triangles of the ternary phase diagram.

The objective of this work has been to validate the concept of TPPP. The Ti–B–C system, for which the ternary phase diagram delineating the various compatibility triangles is shown in Fig. 2(b), was investigated. This diagram has been modified from the one given in Ref. 13, to reflect the presence of the Ti_3B_4 phase that has been discovered more recently[14,15] and the results obtained in this work. This system was chosen because TiC_x has a wide range of stoichiometry and its yield point has been shown to be a strong function of x. For example, the yield stress in compression at 1200°C was found to drop from ≈430

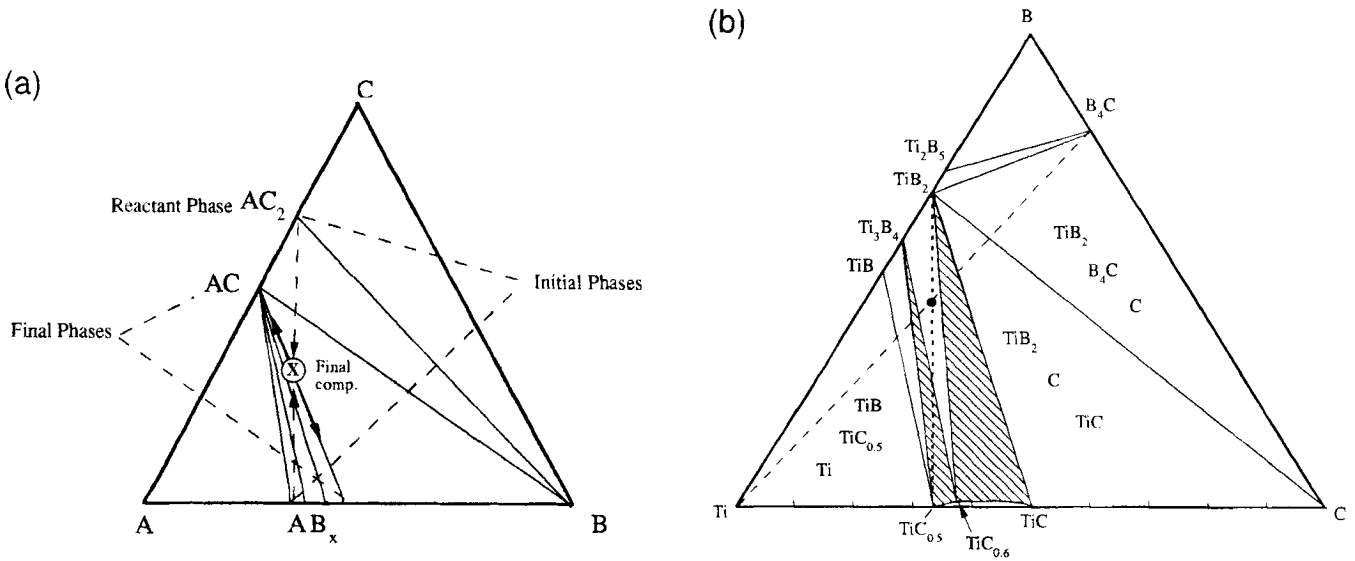

Fig. 2. (a) General reaction scheme for TPPP. AB_x is transient plastic phase defined in text. (b) Compatibility triangles in the Ti–B–C ternary at 1600°C as determined from the work. Shaded areas represent two phase fields. Filled circle represents starting and final composition.

MPa to less than 65 MPa as x decreases from 0.93 to 0.66.[16] Four phases exist along the Ti–B binary, namely, Ti_2B_5, TiB_2, Ti_3B_4, and TiB.

III. Experimental Procedure

High-purity titanium (−325 mesh, 4N purity, Alta Group, Fombell, PA) and B_4C (−325 mesh, ESK, West Germany) powders (Fig. 3) were mixed in either a 3:1 or 4:1 molar ratio and will henceforth be referred to as 3:1 and 4:1, respectively. The Ti powder was an angular hydride–dehydride powder with a 12-μm average agglomerate size. From X-ray diffraction line broadening, however, the average particle size was calculated to be ≈10 nm. The average particle size of the starting B_4C powder was 5 μm and varied from 0.5 to 9 μm. X-ray diffraction indicated that graphite was an impurity phase. Using X-ray calibration curves the volume fraction of the graphite in the starting B_4C was estimated to be ≈10 mol%. In the reactions that follow, for the sake of simplicity, the excess C will be ignored and it will be assumed that the starting composition was B_4C.

The powders were wet ball-milled with alumina grinding media in polyethylene containers for 24 h in 2-propanol and dried under vacuum at room temperature. The dried mixture was V-blended in a sealed container for 12 h, and then cold compacted at 400 MPa into 6.9 cm × 1.2 cm × 0.5 cm bars. The green densities ranged from 65% to 68% for the 3:1 composition and from 73% to 75% for the 4:1 composition; with the higher metal content of the 4:1 composition clearly enhancing the green density. Two green bars of the same composition were placed side by side in a 2.54 cm × 7.62 cm graphite die and hot-pressed under vacuum for varying times and temperatures.

The hot pressing was carried out in a vacuum hot press (Vacuum Industries, Inc., Sommerville, MA) at 10^{-4} torr. Although no special precautions, aside from mixing in propanol and sealing the container during V-blending, were taken to ensure that oxygen was not taken into solid solution, the presence of free C in the B_4C, hot pressing under vacuum, and the long holds at intermediate temperatures were deemed sufficient to get rid of most of the oxygen.

In a preliminary set of runs graphite sheets were inserted between the top and bottom of the samples to protect the die and allow for easy release of the samples. This procedure, however, was discontinued when it was realized that TiC-rich surface layers formed as a result of reaction between the Ti and the graphite sheets. In subsequent runs a BN spray (Union Carbide Corp., Cleveland, OH) was used as a mold release instead, which partially eliminated the problem.

As summarized in Table I, the processing conditions were varied, but for most runs consisted of two stages:

(i) Stage 1: The bars were heated at 10°C/min to 750–800°C and held at that temperature for various times.

(ii) Stage 2: The temperature was increased again at 10°C/min to the final temperature that varied between 1400° and 1600°C and held at that temperature for various times (Table I). In some runs the temperature was raised directly to 1600° at 10°C/min. The load was programmed to increase at 11 MPa/h and reach its peak value of 41 MPa, 2 h before the temperature reaches the stage 1 temperature.

After hot pressing, the reaction products were identified by X-ray analysis (Siemens D-500 System, Siemens, Germany) using Cu$K\alpha$ radiation. The phases present on the surface and their relative abundance were found to differ from the interior and thus, in addition to scanning the surface, the specimens were powdered for analysis. The phases reported in Table I were determined from powdered samples. The final density was measured using Archimedes's principle in water.

The microstructural observations were carried out in an SEM on polished and etched cross sections as well as on fractured surfaces. The samples were etched in a mixture of water, HNO_3, and HF in the proportions 5:5:2 for 1 min.

In order to quantify the reaction kinetics a series of different thermal analysis runs on the 3:1 stoichiometric powder mixtures were carried out (DTA 1700, Perkin-Elmer, Norwalk, CT). The samples were heated to various temperatures under Ar at 10°C/min and held at temperature for 10 min. The heating rate was chosen to correspond to the one used during hot pressing. Following each DTA run each sample was analyzed for its phase composition by XRD.

The hot-pressed samples were subjected to a number of preliminary physical and mechanical tests including 4-point bend tests (MTS Ceramic Testing System, Minneapolis, MN) (outer span 4 cm, inner span 2 cm with a crosshead speed of 0.01 mm/s). Samples 3 mm × 3 mm × 45 mm were electron discharge machined from the hot-pressed plates. The samples' surfaces were finished by wet grinding on a 150-grit diamond wheel in a direction parallel to the length of the bars. The tensile face was further ground to a 30-μm finish using diamond paste. The edges were beveled to eliminate edge effects. The hardness was measured with a Vickers diamond indenter using a load of 300 g. The fracture toughness was also estimated from the indentations.[17]

IV. Results and Discussion

Figure 4 shows the X-ray diffraction results of the 3:1 powders that were heated in the DTA. Based on these results the reaction sequence during the heat-up of the 3:1 composition occurs as follows:

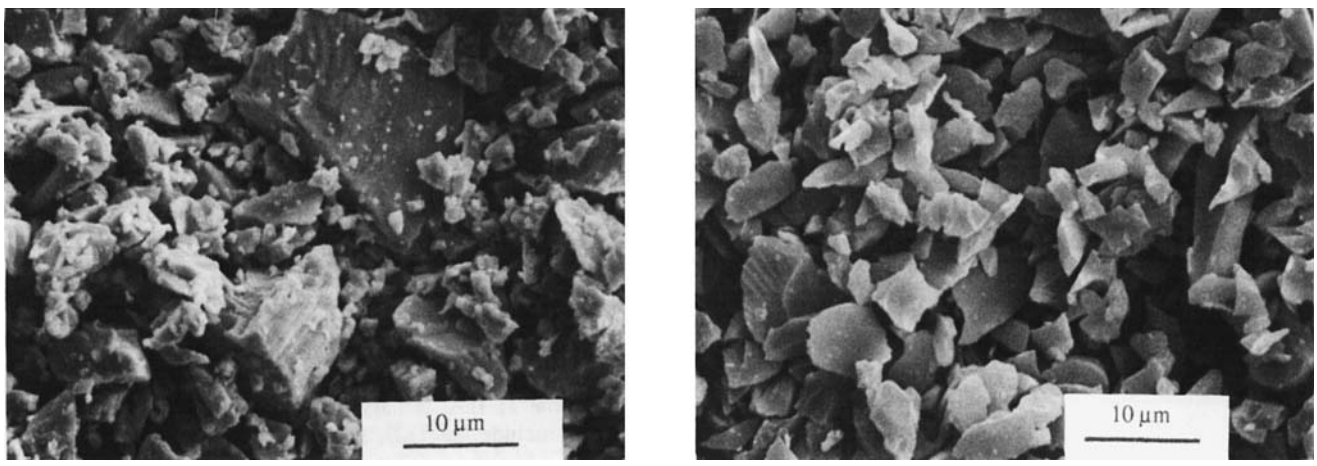

Fig. 3. SEM micrographs of starting powders: (a) Ti, (b) B_4C.

Table I. Summary of Runs

Run no.	Starting stoichiometry	Green density (g/cm³)	Final density* (g/cm³)	Phases present	Processing conditions: State 1 Temp. (°C)	State 1 Time (h)	Stage 2 Temp. (°C)	Stage 2 Time (h)	Pressure (MPa)
1	3:1	2.56 (68%)	2.5 (54%)	TiC, TiB_2			1600	5	0
2	3:1	2.54 (67%)	3.8 (83%)	TiC, TiB_2			1600	5	34
3	3:1	2.52 (66%)	3.4 (86%)	TiC, TiB_2			1600	5	41
4	3:1	2.56	3.69 (86%)	TiC, TiB_2	750	2	1600	2	41
5	3:1	2.55	4.04	TiC, TiB_2	750	4	1600	4	41
6	3:1	2.56	4.15 (90%)	TiC, TiB_2	800	2	1600	4	41
7	3:1	2.54	4.24 (92%)	TiC, TiB_2	800	4	1600	4	41
8	4:1	2.85 (74%)	3.21 (68%)	$TiC_{0.6}, TiB_2, Ti_3B_4$	1600†		1600	5	0
9	4:1	2.84	4.57 (97%)	Ti_3B_4, TiB_2, TiC_x	1600†		1600	4	41
10	4:1	2.86	4.55 (96%)	Ti_3B_4, TiB_2, TiC_x	1600†		1600	5	34
11	4:1	2.83	4.64 (98%)	Ti_3B_4, TiB_2, TiC_x	1600†		1600	5	41
12	4:1	2.85	4.34 (92%)	$TiC_{0.55}, TiB_2, Ti_3B_4$	800	4	1600	0.33	41
13	4:1	2.86	4.69 (99%+)	$TiC_{0.6}, TiB_2, Ti_3B_4$	800	4	1600	4	41

*The theoretical densities of TiC, TiB_2, and Ti_3B_4 were taken to be 4.9, 4.5, and 4.6 g/cm³, respectively. †Heated directly to 1600°C.

$$3Ti + B_4C \rightarrow \tfrac{2}{3}TiB + \tfrac{2}{3}Ti_2B_5 + TiC \quad (3)$$

followed by

$$\tfrac{2}{3}TiB + \tfrac{2}{3}Ti_2B_5 \rightarrow 2TiB_2 \quad (4)$$

the net reaction being

$$3Ti + B_4C \rightarrow 2TiB_2 + TiC \qquad (\Delta V \approx -22\%) \quad (5)$$

and is complete, i.e., TiB and Ti_2B_5 phases disappear, by 1400 K. Thus upon reaching the maximum hot-pressing temperature of 1600°C the only phases present are TiC and TiB_2. The stoichiometry, x, of the TiC_x at that point is >0.95. The overall volume change upon reaction, ΔV, is negative.

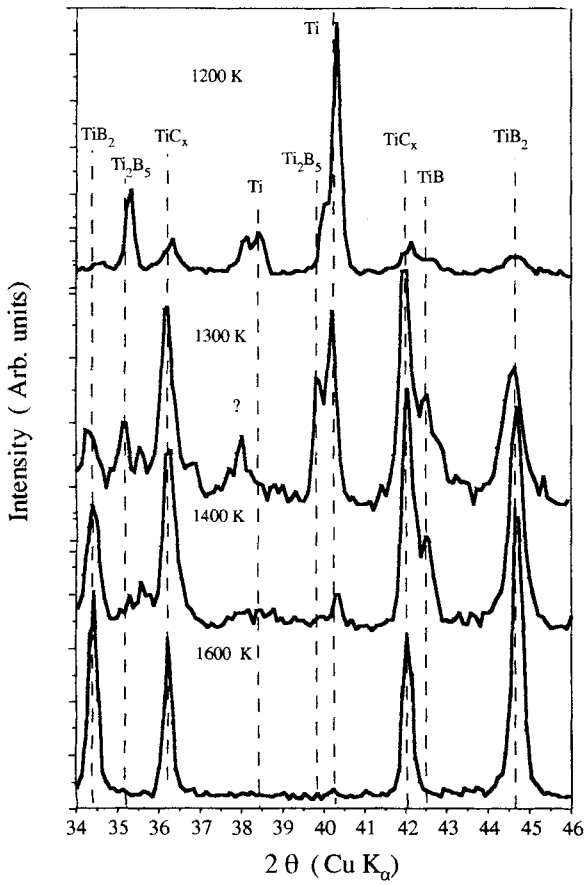

Fig. 4. X-ray diffraction results of 3:1 powders that were heated in the DTA at 10°C/min and held at temperature indicated for 10 min.

The reaction sequence for the 4:1 composition was found to be quite different. From the X-ray diffraction results of the DTA samples and the post-hot-pressed specimens the following observations were made:

(i) The short-duration (10 min) DTA runs resulted in only trace amounts of Ti_3B_4. The phases present at that point were TiB_2 and $TiC_{0.5}$ in roughly the same proportions (Fig. 6(A)).

(ii) The substoichiometry in TiC_x changes from 0.55 to 0.57 (the lattice parameter changes from 3.075 to 3.104 Å; x was related to d using data given in Ref. 13) as the time the composite was held at 1600°C increases from 20 min to 4 h (compare runs 12 and 13).

(iii) After 4 h at 1600°C, the volume fractions of $TiC_{0.6}$, Ti_3B_4, and TiB_2, as determined from the micrographs, were approximately 43%, 25%, and 32%, respectively (Fig. 7).

(iv) The volume fractions of the phases as determined from the areas under the X-ray peaks after hot pressing at 1600°C for 4 h were found to be 17% for Ti_3B_4, 50% $TiC_{0.6}$, and 32% TiB_2. Here it was assumed that the electron densities of the three phases were identical, a reasonable assumption since the X-ray signal is mostly from diffraction from the Ti atoms.

(v) As the intensity of the Ti_3B_4 peaks increased, a concomitant decrease in the TiB_2 peaks was observed (compare Figs. 6(B) and (C)). The fraction of Ti_3B_4 increased from 12% to 17% as the time the composite was held at 1600°C increased from 20 min to 4 h.

Based on these observations the reaction sequence for the 4:1 composition involves the intermediate-phase TiB_2 and occurs in two steps:

$$4Ti + B_4C \rightarrow 2TiB_2 + 2TiC_{0.5} \qquad (\Delta V \approx -13\%) \quad (6)$$

followed by

$$2TiB_2 + 2TiC_{0.5} \rightarrow 0.33Ti_3B_4 + 1.66TiC_{0.57} + 1.33TiB_2 \qquad (\Delta V \approx -3\%) \quad (7)$$

the net reaction at equilibrium being

$$4Ti + B_4C \rightarrow 0.33Ti_3B_4 + 1.66TiC_{0.6} + 1.33TiB_2 \qquad (\Delta V \approx -16\%) \quad (8)$$

The final substoichiometry of the TiC_x as well as the equilibrium number of phases and their relative amounts are linked and depend on where the initial composition (i.e., 4Ti:B_4C) lies in the Ti_3B_4–TiC_x–TiB_2 compatibility triangle. As mentioned above, the Ti–B–C ternary phase diagram reported by Rudy[13] did not include the Ti_3B_4 phase which has since been discovered[14,15] and the existence of which significantly alters the ternary phase diagram at 1600°C. Based on this work, the diagram has been modified as shown in Fig. 2(b). The initial 4:1 composition lies almost halfway along the line joining Ti to B_4C (point

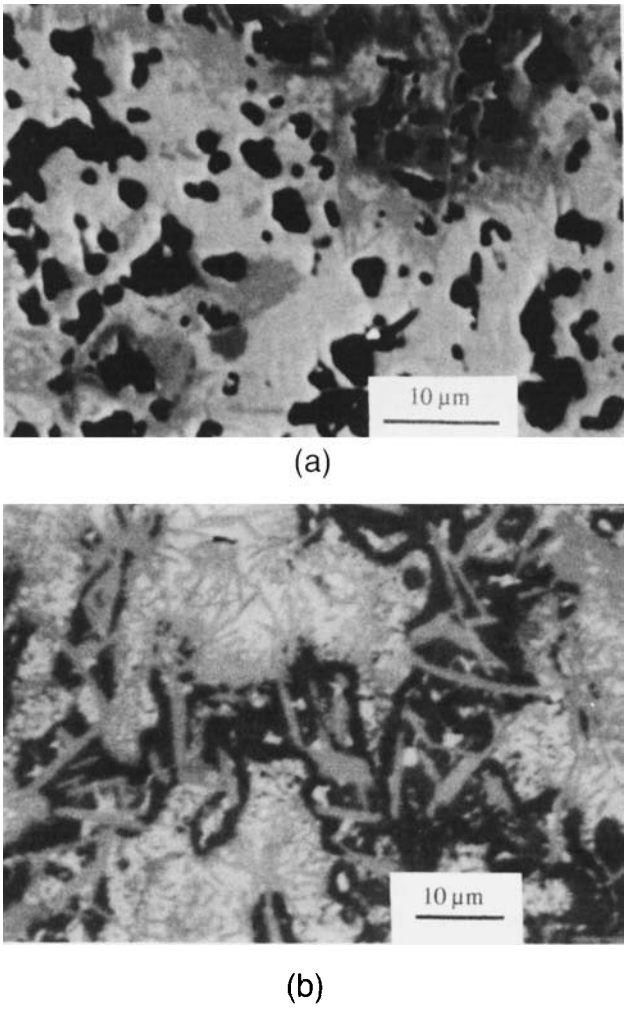

Fig. 5. (a) Backscattered SEM micrograph of 4:1 composite hot-pressed at 1600°C for 20 min (run 12). Density = 92% of theoretical. (b) Backscattered SEM micrograph of 4:1 composite hot-pressed at 1600°C for 4 h (run 13). Density 99% +.

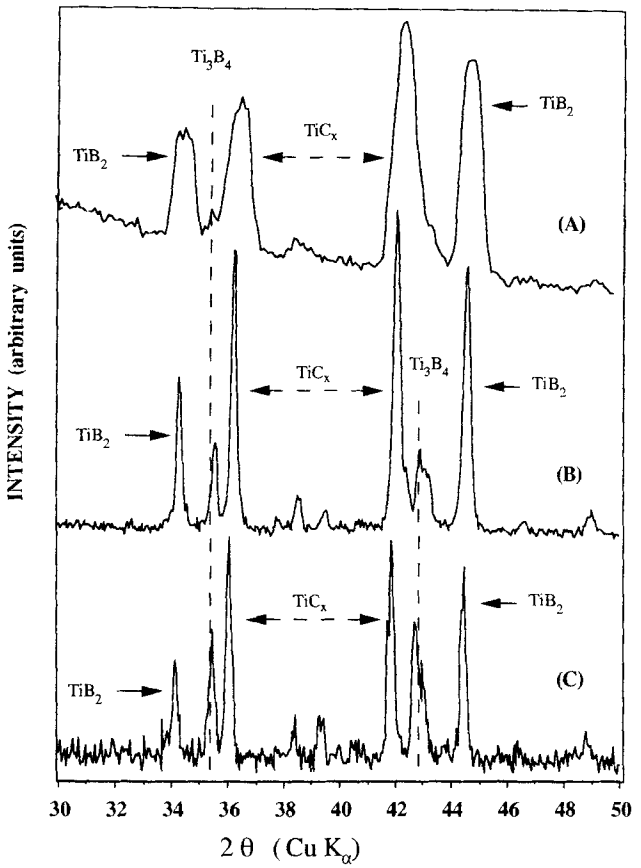

Fig. 6. X-ray diffraction patterns of 4:1 composition for (A) powders heated to 1500°C and held at that temperature for 10 min in DTA, (B) composite shown in Fig. 5(a) (run 12), and (C) composite shown in Fig. 5(b) (run 13).

O in Fig. 2(b)). Upon reaction the line joining Ti to B_4C pivots around point O, to yield TiB_2 and $TiC_{0.5}$ in roughly equal amounts; a conclusion that is supported by the X-ray diffraction results (Fig. 6(A)). Further reaction rotates that line to form Ti_3B_4 and C-rich TiC_x. The Ti_3B_4 forms at the expense of TiB_2, with the extra Ti coming from $TiC_{0.5}$.

The value of x is fixed by the three phases coexisting at equilibrium and the best estimate of that value based on the results obtained above is 0.6. With that value of x, and according to reaction (8), the equilibrium volume fractions of the Ti_3B_4, $TiC_{0.6}$, and TiB_2 are calculated to be 25%, 37%, and 37%, respectively,* in reasonable agreement with the volume fractions of the three phases observed microstructurally (Figs. 5(b) and (7), viz., 25%, 43%, and 32%, respectively. The agreement is even better when it is recalled that the B_4C had some excess C initially. The results are also consistent, within experimental error, with the volume fractions of the phases determined from the area under the various X-ray diffraction peaks, namely, 17% for Ti_3B_4, 50% for $TiC_{0.6}$, and 32% for TiB_2. The lower volume fractions for Ti_3B_4 are most probably due to their preferred orientation as a result of their platelike morphology (see below).

The reason for the slight discrepancy between the value of x determined from the lattice parameter, 0.57, and the value of 0.6 chosen here is not entirely clear. The most probable explanation is that some boron atoms diffused into the TiC_x, forming a solid solution with the latter. In conclusion, the lines joining TiB_2 and Ti_3B_4 to the TiC_x field intersect at $x = 0.6$ (Fig. 2(b)).†

A set of experiments similar to the ones described above are in progress to determine the point at which the TiB and Ti_3B_4 phases intersect the TiC_x field. This value is most probably quite close to $x = 0.5$.

According to the aforementioned reaction sequence, the Ti_3B_4 phase should grow at the expense of the TiB_2, with the extra Ti atom coming from the "Ti-rich" TiC phase. It follows that microstructurally the areas around the Ti_3B_4 should be depleted of the TiB_2 phase. The SEM micrographs (Figs. 5(b) and (7)) unequivocally support this conclusion. Typical backscattered SEM micrographs of 4:1 composites hot-pressed for 20 min and 4 h are shown in Figs. 5(a) and (b), respectively. The corresponding X-ray diffraction patterns are shown in Figs. 6(B) and (C). Three distinct phases are clearly apparent: a long platelike gray phase, a light phase, and a darker phase. In addition to these the porosity in Fig. 5(a) is obvious. The platelike phase was easily identified as Ti_3B_4 since the intensity of the Ti_3B_4 lines correlated with the volume fraction of these plates observed in the SEM micrographs (compare Figs. 5(a) and (b) to corresponding X-ray diffraction patterns shown in Figs. 6(B) and (C)). The light areas are TiC_x which etch differently than the darker B-rich areas (see Fig. 7). Hence the dark areas are most probably pure TiB_2; however, the possibility that they are

*The molar volumes of the Ti_3B_4, TiB_2, and $TiC_{0.6}$ were taken to be 40.64, 15.38, and 12.3, respectively.

†If one assumes that $x = 0.65$, the volume fractions of Ti_3B_4, TiB_2, and TiC_x are calculated to be 34.5%, 30.5%, and 35%, respectively. Similarly if one assumes $x = 0.57$, the respective volume fractions would be 18%, 42%, and 39%. In either case, the agreement with the experimental results is less satisfactory than if x is chosen to be 0.6.

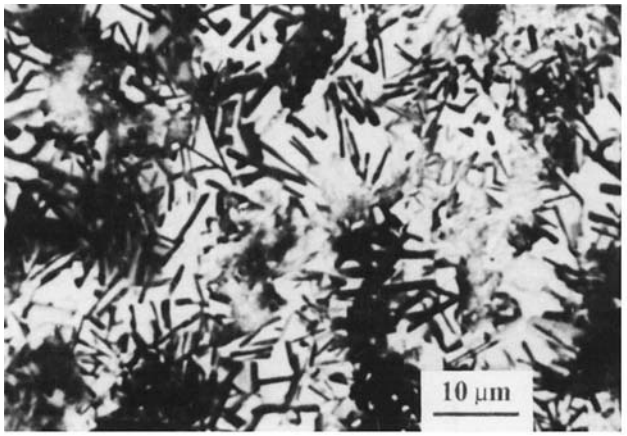

Fig. 7. Backscattered SEM micrograph of etched sample (run 13). Bright areas correspond to $TiC_{0.6}$; the platelike phase is Ti_3B_4. The dark areas are TiB_2.

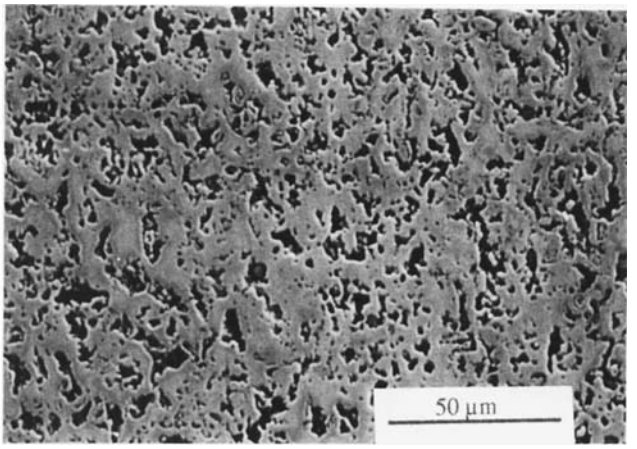

Fig. 9. Typical microstructure of highest-density (92%) 3:1 composite fabricated.The sample was held at 800°C for 4 h and subsequently heated to 1600°C at 10°C/min and held at temperature for 4 h (run 7).

two phase mixtures of TiB_2 and $TiC_{0.5}$ cannot be ruled out at this time. Figure 8 shows a fractured surface which clearly demonstrates the platelike morphology of the Ti_3B_4.

Reaction (6) is quite rapid and is essentially complete after heating the powders to 1500°C at 10°C/min and holding for 10 min. Reaction (7), on the other hand, is quite sluggish. It is the sluggishness of this reaction, and the negligible volume change accompanying it, together with the "softness" of the $TiC_{0.5}$ phase that is believed to be pivotal in obtaining the theoretical densities for this composite. As noted above, the volume change for reaction (6) is $\simeq -13\%$, whereas that for reaction (7) is -3%.

The validity of the concept of transient phase processing is clearly demonstrated when runs 7, 12, and 13 are compared. In each of these runs, upon reaching 1600°C, the predominant phases present were TiB_2 and TiC_x. The difference between runs 7 and 12, however, was in the value of x. For the 3:1 composition (run 7) $x > 0.9$, whereas for runs 12 and 13 $x \approx 0.5$. For the 3:1 composition, 4 h at 1600°C was insufficient to eliminate the volume shrinkage that occurred when reaction (5) took place. The highest final density for this composite was 92%. A typical micrograph for this composite is shown in Fig. 9, where the uniformity of the pores and their small radii are noteworthy. These pores are believed to have developed as a result of the volume change upon reaction. Conversely, for the 4:1 composition the volume changes that occurred when reaction (6) took place were eliminated by the creep and plastic flow of the $TiC_{0.5}$ phase, resulting in a dense final compact. Another critically important factor is the "pinning" of the TiC_x composition at the relatively soft substoichiometry of $x = 0.6$.

Another observation that supports the aforementioned hypotheses is the fact that the surfaces of most samples were porous. It is believed that C diffusion from the graphite dies into the surface layers increased the C content of the TiC_x sufficiently to render it nonplastic and in turn interfered with the densification of the surface.

Comparing runs 1 and 8 with any of the other runs demonstrates the critical importance of applying pressure during the process for densification. When no pressure is applied, the final density after sintering is even less than the initial green density reflecting the effect of the negative volume changes upon reaction on the final density.

It is worth noting that while results presented above do not unambiguously prove the concept of TPPP, since the transient phase was itself a product of a reaction, they strongly support the general validity of the concept. The composition of TiC_x changes from $x = 0.5$ to $x = 0.6$ during the process. We are currently extending the work so as to start with mixtures of TiB_2 and TiC_x of varying x values in an attempt to better model and deconvolute the deformation and reaction mechanisms.

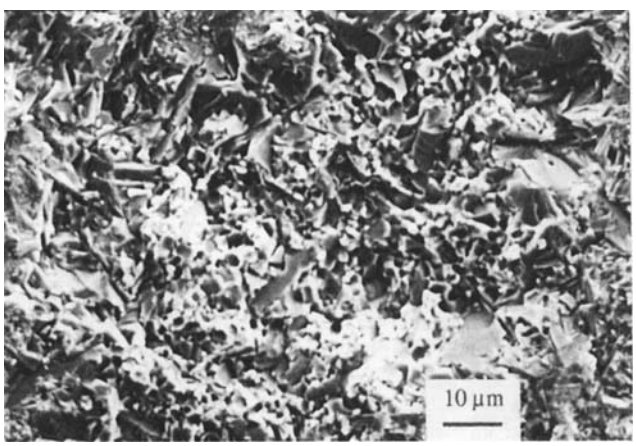

Fig. 8. SEM micrograph of fractured surface of 4:1 composite showing the platelike morphology of Ti_3B_4.

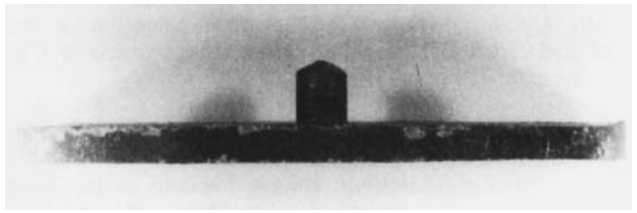

Fig. 10. Photograph of a 4:1 composite that was held at 800°C for 4 h and subsequently heated to 1600°C at 10°C/min and held at temperature for 4 h. The green bar was originally flat. The small protrusion on surface resulted from plastic deformation and creep of Ti and B_4C into a small cylindrical cavity that was present in the upper ram. Actual length of bar is 3 in.

Table II. Summary of Properties Measured for Composites

Composition	Bend strength (MPa)	Fracture toughness ($MPa \cdot m^{1/2}$)*	Hardness (GPa)	Coefficient of thermal expansion† ($°C^{-1}$)
3:1	100 ± 20	4–5	18–24	
4:1	590 ± 30	5.6 ± 0.6	18–30	6.5×10^{-6}

*From indentation. †200–1350°C.

(1) Near Net Shape

Figure 10 is a photograph of a sample of the 4:1 starting composition that was hot-pressed to near theoretical density in two stages (same as run 13). The *initially flat* green compact composed of Ti and B_4C powders was placed in the die in which the ram had a small cylindrical hole in its center. Creep and plastic deformation of the Ti powder at 800°C was sufficient to allow it and the entrained B_4C to flow into the cylindrical cavity. The faithfulness with which the cavity is reproduced given the sharp angles involved are noteworthy. In this respect the Ti metal can be considered to have played the role of a TPP. The large volume changes associated with the reactions, however, partially annul the advantage of having it as a plastic phase. In other words, even if a fully dense specimen were processed at intermediate temperatures, the final composite would still be porous as a result of the large reaction volume changes. Nevertheless, as Fig. 10 makes amply clear, an advantage of starting with metal and ceramic powders is the possibility of exploiting the pre-reaction plasticity of the metal component to form very complex net or near-net shapes prior to reaction. In that respect, the processing of the 4:1 composition involves two TPP processes in succession.

(2) Composite Properties

As noted above a few preliminary measurements were carried out on the 3:1 and 4:1 composites. The results are summarized in Table II (the bend strength values reflect the average of two samples). It is worth noting that these samples were conductive enough to be machined by electron discharge. We are currently extending the measurements to higher temperatures and other properties.

V. Summary and Conclusions

Ceramic/ceramic composites in the Ti–B–C system were fabricated by a process referred to as transient plastic phase processing (TPPP). Starting with Ti and B_4C powders it is possible to *in situ* form fully dense, complex shaped, ultrarefractory ceramic/ceramic composites in the Ti–B–C system, at temperatures as low as 1600°C and moderate pressures (40 MPa).

Two starting compositions of Ti and B_4C were explored: 3:1 and 4:1. The highest density after a 4-h hold at 1600°C for the 3:1 composition was 92%. With the 4:1 composition, on the other hand, fully dense composites comprised of $TiC_{0.6}$, TiB_2, and Ti_3B_4 were fabricated. The attainment of full density for the 4:1 composition is believed to be due to the presence of an intermediate metastable phase that is relatively "soft," here termed the transient plastic phase. The creep and plastic deformation of that phase accommodates the large volume changes accompanying the reaction resulting in dense composites. The absence of such a phase, as in the case of the 3:1 composition, resulted in a porous final composite. Upon reaction, the composition of the transient phase shifts toward a more refractory composition.

At 1600°C Ti_3B_4 and TiB_2 are in equilibrium with $TiC_{0.6}$. These three phases define a compatibility triangle in the Ti–B–C system.

References

[1]J. Ramberg, C. Wolfe, and W. Williams, "Resistance of TiB_2 to High Temperature Yielding," *J. Am. Ceram. Soc.*, **68,** C-78–C-79 (1985).

[2]W. S. Williams, "Influence of Temperature, Strain Rate, Surface Condition and Composition on the Plasticity of Transition-Metal Carbide Crystals," *J. Appl. Phys.*, **35,** 1329–38 (1964).

[3]I. I. Spivak, R. A. Andrievskii, V. V. Klimenko, and V. D. Lazarenko, "Creep in the Binary System TiB_2–TiC and ZrB_2–ZrN," *Sov. Powder Metall. Met. Ceram., (Engl. Transl.)*, **137,** 617–20 (1974).

[4]H. R. Baumgartner and R. A. Steiger, "Sintering and Properties of Titanium Diboride Made from Powder Synthesized in a Plasma-Arc Heater," *J. Am. Ceram. Soc.*, **67,** 207–12 (1984).

[5]H. Pastor, "Metallic Borides: Preparation of Solid Bodies-Sintering Methods and Properties of Solid Bodies"; pp. 475–93 in *Refractory Borides*. Edited by V. I. Malkovich. Springer Verlag, New York, 1977.

[6]C. F. Yen, C. S. Yust, and G. W. Clark, "Enhancement of Mechanical Strength in Hot-Pressed TiB_2 Composites by the Addition of Fe and Ni," Rept. No. CONF-781093-2, Oak Ridge National Lab, Oak Ridge, TN, 1978.

[7]T. Watanabe and S. Kouno, "Mechanical Properties of TiB_2–CoB–Metal Boride Alloys," *Am. Ceram. Soc. Bull.*, **61** [9] 970–73 (1982).

[8]J. Crider, "Self-Propagating High Temperature Synthesis—A Soviet Method for Producing Ceramic Materials," *Ceram. Eng. Sci. Proc.*, **3** [9–10] 519–28 (1982).

[9]J. W. McCauley, N. D. Corbin, T. Resetar, and P. Wong, "Simultaneous Preparation and Self-Sintering of Materials in the System Ti–B–C," *Ceram. Eng. Sci. Proc.*, **3** [9–10] 538–54 (1982).

[10]W. B. Johnson, T. D. Claar, and G. H. Schiroky, "Preparation and Processing of Platelet-Reinforced Ceramics by the Directed Reaction of Zirconium with Boron Carbide," *Ceram. Eng. Sci. Proc.*, **10** [7–8] 588–98 (1989).

[11]M. Sacks, N. Bozkurt, and G. Schieffele, "Fabrication of Mullite and Mullite-Matrix Composites by Transient Viscous Sintering of Composite Powders," *J. Am. Ceram. Soc.*, **74** [10] 2428–37 (1991).

[12]R. Roy and W. McDonough, "Intrinsic Volume Changes of Self-Propagating Synthesis," *J. Am. Ceram. Soc.*, **68** [5] C-122–123 (1985).

[13]E. Rudy, "Ternary Phase Equilibria in Transition Metal–Boron–Carbon–Silicon Systems, Part V," AFML-TR-65-2, Air Force Materials Laboratory, Wright-Patterson Air Force Base, Ohio, 1965.

[14]R. G. Fenish, "A New Intermediate Compound in the Ti–B System, Ti_3B_4," *Trans. Metall. Soc. AIME*, **236,** 804 (1966).

[15]K. Spear, P. McDowell, and F. McMahon, "Experimental Evidence for the Existence of the Ti_3B_4 phase," *J. Am.Ceram. Soc.*, **69** [1] C-4–C-5 (1986).

[16]D.Miracle and H. Lipsitt, "Mechanical Properties of Fine-Grained Substoichiometric TiC," *J. Am. Ceram. Soc.*, **66** [8] 592–96 (1983).

[17]A. G. Evans and A. E. Charles, "Fracture Toughness Determinations by Indentation," *J. Am. Ceram. Soc.*, **59** [7–8] 371–72 (1976). □